

Freestanding microscale 3D polymeric structures with biologically-derived shapes and nanoscale features

Christopher S. Gaddis and Kenneth H. Sandhage^{a)}

*School of Materials Science and Engineering, Georgia Institute of Technology,
Atlanta, Georgia 30332*

(Received 25 May 2004; accepted 2 June 2004)

Microscale polymeric structures with intricate three-dimensional (3D) shapes and nanoscale features were synthesized by using silica-based microshells of diatoms (unicellular algae) as transient scaffolds. Diatom microshells were immersed in dilute solutions of polymer precursors in volatile solvents. After extraction and solvent evaporation, the resulting thin films on the microshells were cross-linked to form rigid polymer coatings. Selective silica dissolution then yielded freestanding polymeric structures that retained the microshell shapes and fine features. By utilizing bioscaffolds capable of genetically precise and massively parallel replication, enormous numbers of polymeric micro/nanostructures with identical 3D shapes may be generated for various applications.

Significant global effort is underway to develop shape-tailored polymeric microstructures with fine (down to nanoscale) features for medical, cosmetic, aerospace, environmental, agricultural, optical, fluidic, and microelectromechanical applications.^{1–10} Microfabrication routes based on layer-by-layer two-dimensional (2D) techniques, such as lithographic micromachining methods developed for the silicon microelectronics industry, are not particularly well suited for fabricating three-dimensional (3D) polymeric structures with complex shapes (e.g., curved 3D surfaces) and with very fine (down to nanoscale) features.^{11,12} However, alternative approaches capable of direct 3D micro/nanofabrication must also be scalable to allow for high-throughput production.¹² The often-conflicting requirements of precise 3D fabrication on a fine scale and continuous production on a large scale may be achieved through self-assembly processes.

Nature is particularly adept at massively parallel nanoscale self-assembly. Numerous examples exist of natural microorganisms that direct the assembly of mineralized (bioclastic) nanoparticle-based structures with complex, but reproducible 3D shapes.^{13–17} Among the best-known and most striking examples are diatoms. Diatoms are single-celled algae that populate virtually every body of water on earth.^{16,17} Diatoms possess rigid cell walls

(frustules) composed of amorphous silica nanoparticles.¹⁸ Each diatom species assembles a frustule with a unique 3D shape and with well-controlled patterns of fine features (pores, channels, and protuberances).^{16–18} Such morphological specificity is a strong indication that the frustule assembly process is under genetic control.¹⁹ The maximum dimensions of such frustules can range from $<1\ \mu\text{m}$ to $>10^2$ microns, whereas the fine, regular features distributed on the frustule wall possess characteristic dimensions of 10^1 – 10^2 nanometers.^{16,17} A wide diversity in frustule shapes and features can be found among the tens of thousands of diatom species that are known to exist, as is illustrated in the secondary electron images in Fig. 1.^{16,20} Sustained reproduction (repeated doubling) of a given diatom species can yield enormous numbers of descendant diatoms with similarly shaped frustules (e.g., 40 sustained reproduction cycles would yield 2^{40} or more than 1 trillion frustules of similar geometry).²¹

We demonstrate here, for the first time, that freestanding 3D polymeric structures with maximum dimensions on the microscale (tens of microns) and fine features on the nanoscale (10^1 – 10^2 nm) can be generated by using: (i) diatom frustules as transient scaffolds, and (ii) a solution-coating process involving dilute solutions of polymer precursors dissolved in volatile solvents. Although biomineralized scaffolds have been used to synthesize polymeric, ceramic, or composite structures, such prior work has involved scaffolds with sizes and characteristic features that were several orders of magnitude larger than that for diatom frustules (e.g., 10^0 – 10^1 mm coral scaffolds with 10^1 – 10^2 micron diameter pore channels).^{22,23}

^{a)}Address all correspondence to this author.

e-mail: ken.sandhage@mse.gatech.edu

DOI: 10.1557/JMR.2004.0342

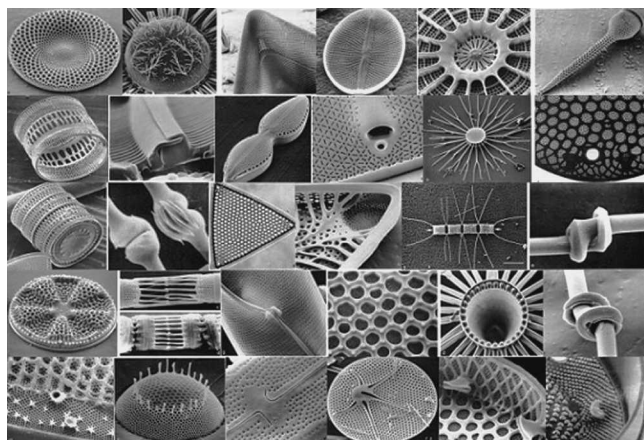
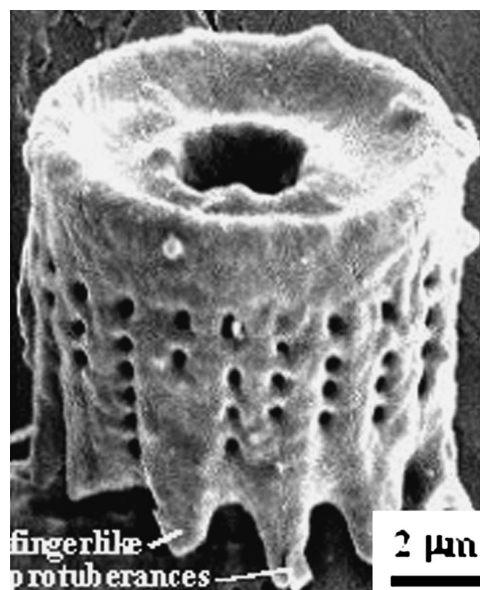


FIG. 1. Secondary electron images of silica-based microshells (frustules) of several diatom species (assembled by M. Hildebrand, Univ. California at San Diego, from images in Ref. 16; reprinted with the permission of Cambridge University Press).

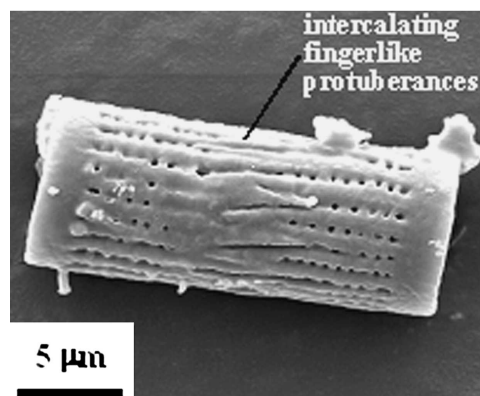
The fine-size scales of diatom frustules, wide range of available frustule shapes among the various extant diatom species, and genetically precise and massively parallel manner in which a given frustule shape can be replicated (via sustained reproduction of a given diatom species) make these nanoparticle structures particularly attractive as 3D micro/nanoscaffolds. The scalable solution-coating process developed in this work enables such intricate biologically derived shapes and fine (nanoscale) features to be preserved as polymeric structures.

Scanning electron microscope images of the diatom frustules (obtained as diatomaceous earth filter material from a local vendor) used as transient scaffolds in this work are shown in Fig. 2. These frustules possessed hollow cylindrical shapes with diameters of 8–12 μm . Some of the frustules possessed an end with a circular hole and a protruding outer rim, as shown in Fig. 2(a). The other end of these frustules was closed and possessed fingerlike protuberances. The fingerlike protuberances from one cylinder were often observed to intercalate with those of another to form larger, paired assemblies, as is shown in Fig. 2(b). Other frustules, such as shown in Fig. 2(c), were observed to have closed ends. The side walls of each of the frustules contained mesoscale pores (diameters of several hundred nanometers) arranged in rows running parallel to the cylinder length.

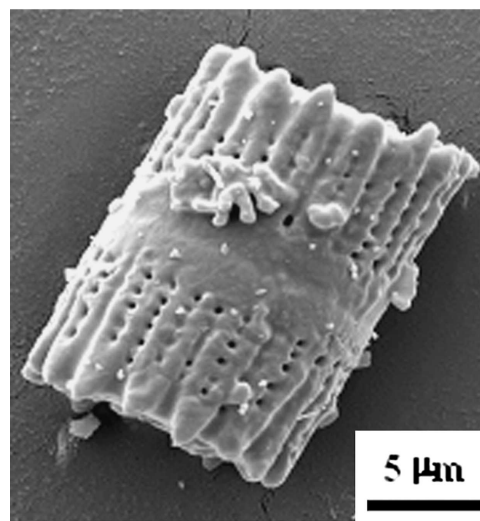
Polymer coatings were applied by immersing the diatom frustules in polymer precursor solutions. Prior to immersion, the diatom frustules were rinsed with distilled water and acetone to remove residual salts and/or oils. The coating solution contained a two-part, 5 min curing epoxy mixture (Loctite Quick Set Epoxy Gel, Henkel Consumer Adhesives, Inc., Avon, OH). The initial coating solution consisted of 10 wt% of this quick-curing epoxy mixture dissolved in acetone. One gram of diatom frustules was then added to 30 ml of this epoxy/



(a)



(b)



(c)

FIG. 2. (a, b, c) Secondary electron images of silica-based diatom frustules used as transient scaffolds.

acetone solution. The mixture was stirred for 15 min and the diatom frustules were then removed from the solution by filtration. The acetone was allowed to evaporate, and the epoxy coating was allowed to cure at room temperature. The coated frustules were then immersed in an aqueous solution containing 49 wt% hydrofluoric acid to selectively dissolve the underlying silica from the coating (note: upon removal of the silica, the specimens were observed to float in the HF solution). After washing with distilled water, the specimens were dispersed in ethanol and then applied by dropper to an electron microscope stub. After the ethanol was allowed to evaporate, the specimens were coated with a thin layer of gold to avoid charging in the electron microscope. A representative secondary electron image of the resulting specimen is shown in Fig. 3(a). With this coating approach, continuous coverage of the internal and external surfaces was achieved. However, the epoxy coating was sufficiently thick enough for the mesoscale pores to be completely filled in and covered over. The continuous coating and the filled pores are clearly revealed in the secondary electron images of a partially fractured specimen shown in Figs. 3(b) and 3(c).

To reduce the coating thickness (and thereby preserve the finer frustule features), the concentration of the epoxy in the solution with acetone was reduced from 10 to 7 wt%. After polymerization and then selective dissolution of the silica in the HF solution, the epoxy structures shown in Figs. 4(a) and 4(b) were obtained. Through the use of a more dilute epoxy solution, these structures retained the mesoscale pores and fine features of the starting diatom frustules. Indeed, the structures shown in Figs. 4(a) and 4(b) were quite similar in morphology to the starting frustule structures shown in Figs. 2(a) and 2(c). Thermogravimetric (TG) analyses were conducted on these specimens in air at a heating rate of 10 °C/min (TGA 7, Perkin Elmer Inc., Boston, MA). TG analysis of the coated specimens prior to silica dissolution revealed that the epoxy coating comprised 28.6% of the weight of the specimen. After exposure of the silica to the HF solution, TG analysis [Fig. 5(a)] confirmed that all of the silica had been removed. EDX analyses of a starting diatom frustule and an epoxy replica are shown in Figs. 5(b) and 5(c), respectively. In Fig. 5(c), the presence of a strong carbon peak and the loss of the strong Si peak relative to Fig. 5(b) were consistent with the conversion of the silica-based diatom frustule into an epoxy replica. The aluminum peaks in Figs. 5(b) and 5(c), and the small silicon peak in Fig. 5(c) were generated by the aluminum alloy stub onto which the specimens were placed. The small fluorine peak in Fig. 5(c) was a result of residual fluorine from HF treatment, and the small gold peak in Fig. 5(c) was due to a gold coating applied to minimize charging in the electron microscope.

This work demonstrates that freestanding microscale

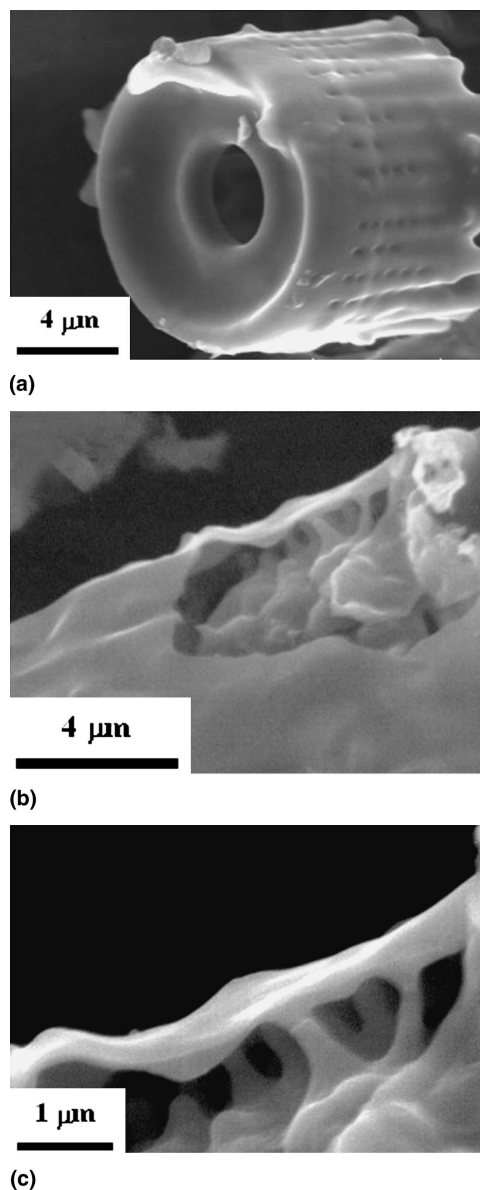
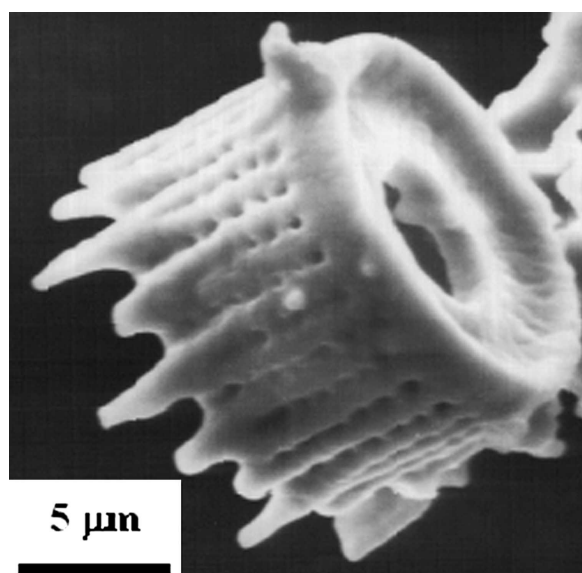
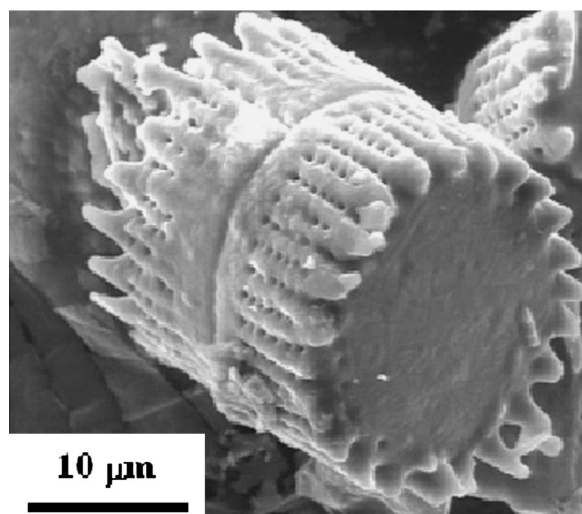


FIG. 3. Secondary electron images of epoxy structures derived from diatom frustule scaffolds (after immersion in a 10 wt% epoxy solution, curing at room temperature, and silica dissolution in a hydrofluoric acid solution). Lower and higher magnification images of a fractured section of an epoxy structure are shown in (b) and (c), respectively.

polymeric structures with complex 3D shapes and nanoscale features may be synthesized by using the frustules of self-replicating diatoms as transient scaffolds. Although a wide variety of frustule shapes exist among the various diatom species, the coating process described in this paper is not limited to the use of only these bioclastic structures. Nature provides numerous other self-replicating biomineralized micro/nanostructures with multifarious 3D shapes (e.g., the microshells of coccolithophorids, silicoflagellates, radiolarians, sponges, bacteria, etc.^{13–15,24}) that may be utilized to generate polymer structures of desired morphology. Furthermore,



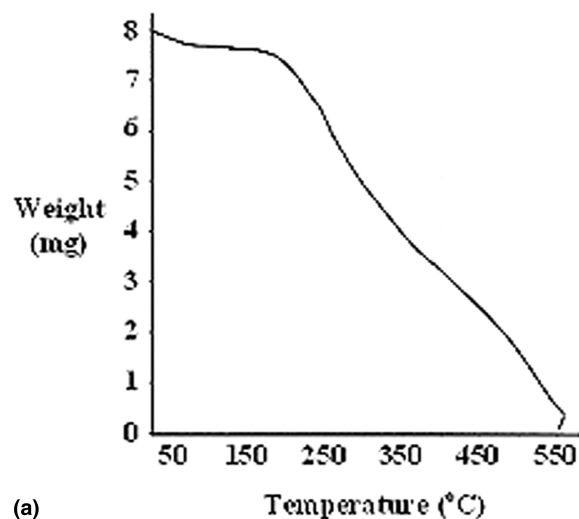
(a)



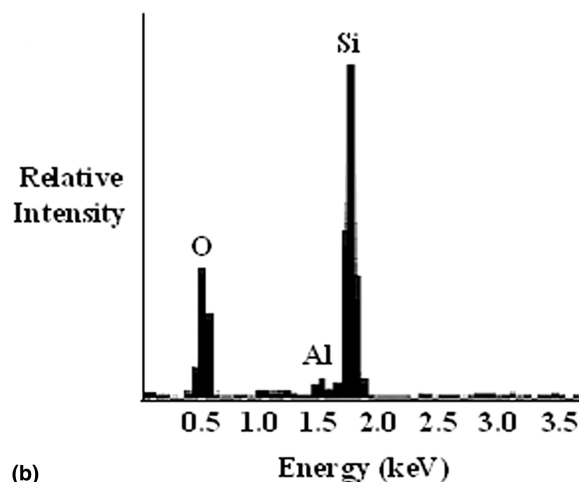
(b)

FIG. 4. (a, b) Secondary electron images of epoxy structures derived from diatom frustule scaffolds (after immersion in a 7 wt% epoxy solution, curing at room temperature, and silica dissolution in a hydrofluoric acid solution).

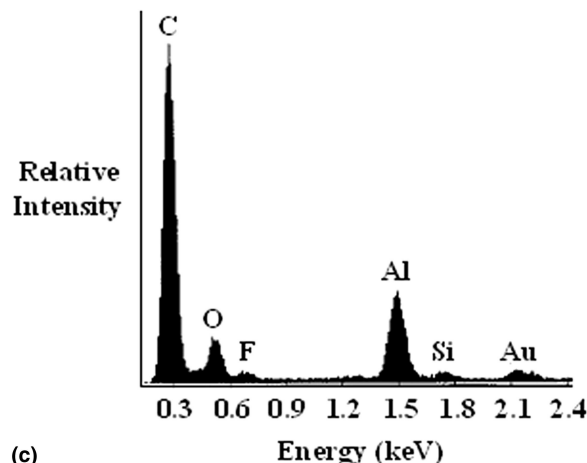
the genetic engineering of diatoms or other biomineralizing organisms may lead to a variety of replicable bioscaffolds with non-natural shapes (note: toward this end, the genome of a diatom, *Thalassiosira pseudonana*, has recently been mapped²⁵). The chemistries of the structures generated by the present process are also not limited to epoxy-based compositions. A variety of organic micro/nanostructures may be generated from bioclastic scaffolds provided that (i) a dilute solution of the organic material, or a precursor to the organic material, can be dissolved in a volatile solvent, (ii) a continuous organic film can be produced by infiltration of the solution into, and deposition onto, the scaffold and then evaporation of



(a)



(b)



(c)

FIG. 5. (a) Thermogravimetric analysis of epoxy replicas (after silica removal) of diatom frustules. Energy dispersive x-ray analyses of (b) a starting diatom frustule and (c) an epoxy replica of a diatom frustule.

the solvent, and (iii) the underlying bioclastic scaffold can be selectively removed from the organic coating (e.g., by selective dissolution in an acidic solution). For the latter requirement, the organic coating must remain

intact as the bioclastic scaffold is removed, which may necessitate an additional processing step (e.g., cross-linking of a polymer coating prior to dissolution of the scaffold). Unlike other approaches for fabricating 3D polymeric micro/nanostructures, this solution-based bioscaffold coating process does not require expensive patterning facilities or reaction processing equipment and is highly scalable. The bioscaffolds may also be cultured in large quantities. Indeed, large-scale diatom cultivation is currently used in aquaculture operations (i.e., diatoms provide a food source for the commercial production of clams, oysters, scallops, shrimp, and several fish species).²⁶ Scale up of the present process could enable the generation of large quantities of inexpensive, 3D polymer micro/nanostructures for use in a host of biomedical, agricultural, cosmetic, environmental, chemical/catalytic, microfluidic, gas sensing, photonic, and aerospace applications.¹⁻¹²

ACKNOWLEDGMENTS

This work was supported by the Air Force Office of Scientific Research (Dr. Joan Fuller, Program Manager). Helpful discussions with Dr. Zhongren Yue (Department of Materials Science and Engineering, University of Illinois) on polymer formulations are gratefully acknowledged.

REFERENCES

1. Y. Yang, C. Zeng, and L.J. Lee: Three-dimensional assembly of polymer microstructures at low temperatures. *Adv. Mater.* **16**, 560 (2004).
2. D.K. Armani and C. Liu: Microfabrication technology for polycaprolactone, a biodegradable polymer. *J. Micromech. Microeng.* **10**, 80 (2000).
3. L.P. Lee, S.A. Berger, D. Liepmann, and L. Pruitt: High aspect ratio polymer microstructures and cantilevers for bioMEMS using low energy ion beam and photolithography. *Sens. Actuators A* **71**, 144 (1998).
4. M. Seiller, M-C. Martini, and S. Benita: Cosmetic applications of vesicular delivery systems, in *Microencapsulation: Methods and Industrial Applications*, edited by S. Benita (Marcel Dekker, New York, 1996), p. 588.
5. T-B. Xu, J. Su, and Q. Zhang: Electroactive-polymer-based MEMS for aerospace and medical applications. *SPIE Proc.* **5055**, 66 (2003).
6. A. Markus: Advances in the technology of controlled-release pesticide formulations, in *Microencapsulation: Methods and Industrial Applications*, edited by S. Benita (Marcel Dekker, New York, 1996), p. 73.
7. J-S. Heo, N-H. Park, J-H. Ryu, G-H. Choi, and K.D. Suh: Novel light emitting diode using organic electroluminescence microcapsules. *Macromol. Chem. Phys.* **204**, 2002 (2003).
8. M.P. Joshi, H.E. Pudavar, J. Swiatkiewicz, P.N. Prasad, and B.A. Reianhardt: Three-dimensional optical circuitry using two-photon-assisted polymerization. *Appl. Phys. Lett.* **74**, 170 (1999).
9. C.H. Ahn: Development of polymer MEMS structures for microfluidic devices and lab-on-a-chips. *Polymer Preprints* **44**, 530 (2003).
10. S. Ballandras, M. Calin, S. Zissi, A. Bertsch, J.C. Andre, and D. Hauden: Microstereolithography and shape memory alloy for the fabrication of miniaturized actuators. *Sens. Actuators A* **62**, 741 (1997).
11. V.K. Varadan and V.V. Varadan: Micro stereo lithography and fabrication of 3D micro devices. *SPIE Proc.* **3879**, 116 (1999).
12. O. Rotting, W. Ropke, H. Becker, and C. Gartner: Polymer microfabrication technologies. *Microsystem Technologies* **8**, 32 (2002).
13. E. Bauerlein: Biomineralization of unicellular organisms: An unusual membrane biochemistry for the production of inorganic nano- and microstructures. *Angew. Chem. Int. Ed. Engl.* **42**, 614 (2003).
14. J.C. Weaver, L.I. Pietrasanta, N. Hedin, B.F. Chmelka, P.K. Hansma, and D.E. Morse: Nanostructural features of demosponge biosilica. *J. Struct. Biol.* **144**, 271 (2003).
15. S. Mann: Molecular tectonics in biomineralization and biomimetic materials chemistry. *Nature* **365**, 499 (1993).
16. F.E. Round, R.M. Crawford, and D.G. Mann: *The Diatoms: Biology & Morphology of the Genera* (Cambridge University Press, Cambridge, U.K., 1990).
17. E.L. Duke and B.E.F. Reimann: The Ultrastructure of the Diatom Cell, in *The Biology of Diatoms*, edited by D. Werner (Blackwell Scientific Publications, Oxford, U.K., 1977), p. 65.
18. S.A. Crawford, M.J. Higgins, P. Mulvaney, and R. Wetherbee: Nanostructure of the diatom frustule as revealed by atomic force and electron microscopy. *J. Phycol.* **37**, 543 (2001).
19. M. Hildebrand and R. Wetherbee: Components and control of silicification in diatoms, in *Progress in Molecular and Subcellular Biology*, edited by W.E.G. Muller (Springer-Verlag, Berlin, Germany, 2003), Vol. 33, p. 11.
20. D.G. Mann and S.J.M. Droop: Biodiversity, biogeography, and conservation of diatoms. *Hydrobiologia* **336**, 19 (1996).
21. V. Martin-Jezequel, M. Hildebrand, and M.A. Brzezinski: Silicon metabolism in diatoms: Implications for growth. *J. Phycol.* **36**, 821 (2000).
22. J.N. Weber and E.W. White: Raplamineform: A new process for preparing porous ceramic, metal, and polymer prosthetic materials. *Science* **176**, 922 (1972).
23. D.P. Skinner, R.E. Newnham, and L.E. Cross: Flexible composite transducers. *Mater. Res. Bull.* **13**, 599 (1978).
24. H.A. Lowenstam and S. Weiner: Mineralization by organisms and the evolution of biomineralization. In *Biomineralization and Biological Metal Accumulation*, edited by P. Westbroek and E.W. de Jong (D. Reidel Publishing Co., Hingham, MA, 1983), p. 191.
25. Joint Genome Institute website: <http://genome.jgi-psf.org/thaps1/thaps1.home.html>
26. T. Lebeau and J-M. Robert: Diatom cultivation and biotechnologically relevant products. Part I. Cultivation at various length scales. *Appl. Microbiol. Biotechnol.* **60**, 612 (2003).